Spectroscopic investigation of the copper (I)-rich phosphate $CuZr_2(PO_4)_3$

1992 J. Phys.: Condens. Matter 4 3031

(http://iopscience.iop.org/0953-8984/4/11/026)

J. Phys.: Condens. Matter 4 (1992) 3031–3042. Printed in the UK

Spectroscopic investigation of the copper (I)-rich phosphate $CuZr_2(PO_4)_3$

P Boutinaud†, C Parent†, G Le Flem†, C Pedrini‡ and B Moine‡

† Laboratoire de Chimie du Solide du CNRS, 351 Cours de la Libération, 33405 Talence Cédex, France

‡ Unité de Recherche Associée 442 du CNRS, Laboratoire de Physico-chimie des Matériaux Luminescents, Université Lyon I, 43 Boulevard du 11 Novembre, 69622 Villeurbanne, France

Received 14 October 1991

Abstract. The Nasicon-type phosphate $CuZr_2(PO_4)_3$ exhibits two fluorescences occurring in the violet and green regions. They are assigned to two different centres: the violet one to isolated Cu^+ and the green one to Cu^+–Cu^+ pairs occupying the same site. These assignments are in agreement with previous structural investigations using x-ray, neutron and EXAFS measurements and provide information about the location of copper ions in the crystal. A third luminescence is detected in the blue range at low temperature. The origin of this fast, strong emission is not clearly established. It could be due to Cu^+–Cu^0 pairs in the M(1) site.

1. Introduction

The spectroscopic properties of copper-doped alkali halides [1–5] and glasses [6–10] have been intensively investigated. In these systems the fluorescence mechanism involves a $3d^9 4s \rightarrow 3d^{10}$ transition strictly forbidden for the free-ion but partially coupled in crystal or glasses with lattice vibrations of odd parity. The fluorescence spectra have the appearance of a single broad band peaking either in the UV range for the alkali halides or in the visible range for glasses. The broad band emission exhibited by the latter materials is characteristic of Cu^+ occupying a large variety of sites.

The first copper-rich fluorescent insulator $CuZr_2(PO_4)_3$ was discovered in 1987 [11]. Its crystal structure was investigated in detail using x-ray and neutron powder diffraction [12], and also x-ray absorption spectroscopy (EXAFS) [13]; and is of the Nasicon type. The Cu^+ ions are localized in an off-centre position of the commonly labelled M(1) site, which is an oxygenated elongated antiprism. The copper environment can be described as a compromise between the usual linear coordination found in several copper (I) oxides (e.g. Cu_2O) and the geometry of the M(1) site created by the covalent $[Zr_2(PO_4)_3]$ framework. Two short copper–oxygen distances of about 2 Å were actually measured. An EXAFS analysis revealed the existence of a relatively large proportion of M(1) sites simultaneously occupied by two Cu^+ ions, with a rather short Cu–Cu distance of 2.40 Å, i.e. below the interatomic distance in the metal (2.56 Å). Accordingly, the M(1) sites can be completely empty or occupied

0953-8984/92/113031+12$04.50

by one or two copper ions. In addition, both x-ray and neutron studies exclude the presence of copper in the other possible site of the structure, e.g. M(2).

In contrast with the luminescence properties of these systems, three fluorescence bands were observed peaking at 400 nm (violet), 460 nm (blue) and 550 nm (green), respectively. This behaviour leads us to examine a possible role for the $(Cu^+)_2$ copper pairs in the process of luminescence.

The interaction between d^{10} cations within aggregates remains an open question. From a theoretical point of view, the formation of hybridized valence orbitals by introducing an s and p character in the d functions, has been assumed by several authors. Following Mehrotra and Hoffmann [14], a weak but real attractive interaction between the two metallic ions can occur. In this context, the present paper reports a detailed investigation of the luminescence properties of $CuZr_2(PO_4)_3$.

2. Experimental procedure

The samples were prepared as previously described [11]. The emission and excitation spectral distributions were analysed with a Jobin–Yvon HRS 3 monochromator and detected using an R 928 Hamamatsu photomultiplier. The excitation source was a high-pressure xenon lamp emitting between 200 and 1000 nm. Both emission and excitation set-ups were carefully calibrated and the spectra corrected accordingly. The spectrometer was equipped with a liquid helium cryostat for low-temperature measurements.

The fluorescence decays have been recorded using a Q-switched Nd^{3+} YAG pumped-dye-laser beam as an excitation source, which could be doubled or frequency mixed with the fundamental (1.064 μm) for an excitation at around 282 or 320 nm. The emission was dispersed by a Hilger computer scannable monochromator and detected with a Hamamatsu R 1477 PMT followed by an amplifier/discriminator and a photon counter.

Decays longer than 10 μs were recorded with a multichannel analyser (35 Plus model from Canberra) with a minimum dwell time per channel of 200 ns. A Lecroy digital oscilloscope with a 75 ns delay line allows us to record decays shorter than 10 μs. For time-resolved spectroscopy (TRS), the signal was sampled by an Ortec 9320 boxcar equipped with an integrator (model 165).

Excitation spectra in the vacuum UV range were obtained at LURE (University of Orsay) using Super ACO synchrotron radiation as the light source.

3. Experimental results

3.1. Emission spectra

Figure 1 displays the emission spectra obtained under a continuous irradiation at 254 and 320 nm. The choice of these wavelengths will be justified after the excitation spectra have been examined.

Under a 254 nm excitation (broken curve), $CuZr_2(PO_4)_3$ exhibits violet emission ($\lambda_{max} \simeq 410$ nm) at 6.5 K as well as a weak green emission peaking at about 550 nm. As the temperature increases, the half widths of both bands enlarge slightly. Above 150 K, the green-band intensity increases at the expense of the violet band which disappears completely at 230 K (figure 2). The maxima of the two bands are

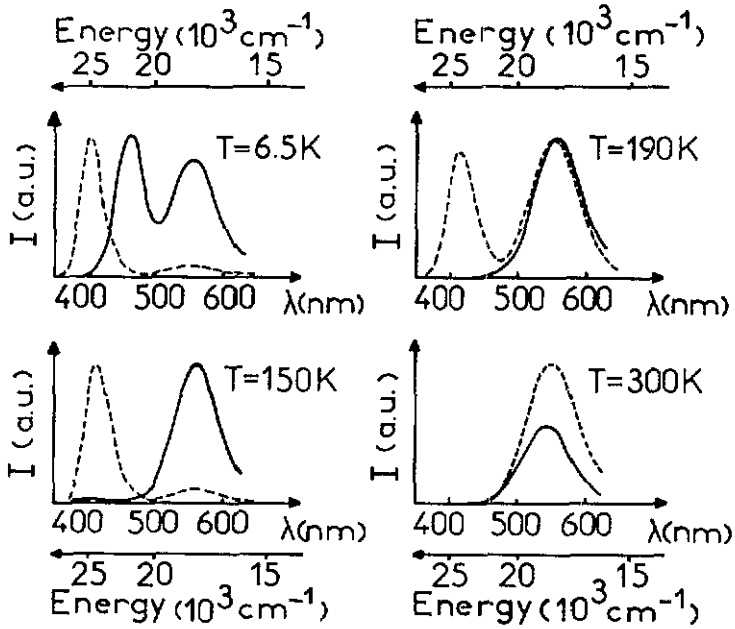

Figure 1. Thermal evolution of $CuZr_2(PO_4)_3$ emission spectral distribution under 254 nm (broken curve) and 320 nm (full curve) continuous excitation.

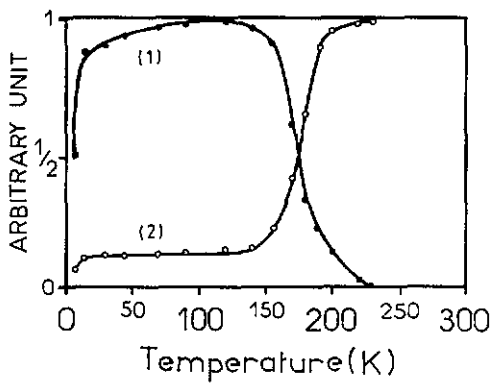

Figure 2. Temperature dependence of the violet (1) and green (2) emission intensities under 254 nm excitation.

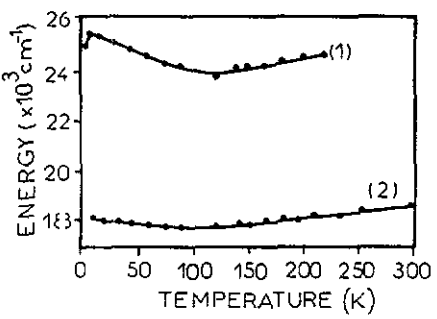

Figure 3. Thermal evolution of the violet (1) and green (2) emission band maximum position.

red shifted between 6.5 K and 130 K and then blue shifted for higher temperatures (figure 3). At 300 K, $CuZr_2(PO_4)_3$ exhibits only green fluorescence.

The violet emission is never observed under a 320 nm excitation. In contrast, at 6.5 K, a new band peaking at 460 nm appears in addition to the green one with a comparable high intensity (figure 1, full curve). The thermal dependence of the relative intensities of both bands is shown in figure 4. These intensities are roughly constant at very low temperatures (below 40 K). Above this temperature, the green

fluorescence increases while the blue one decreases correspondingly. The blue curve suffers thermal extinction at around 80 K.

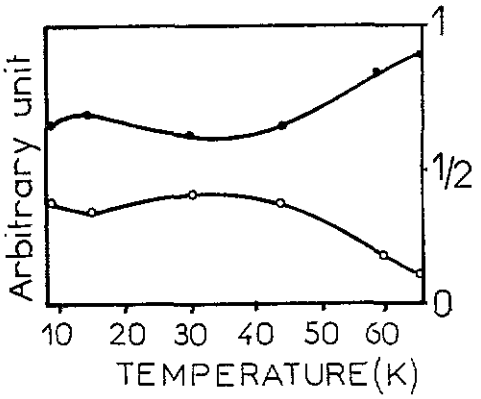

Figure 4. Temperature dependence of the relative intensities of green (●) and blue (○) fluorescences.

3.2. Excitation spectra

Figure 5 represents the spectral distribution of the excitation bands of $CuZr_2(PO_4)_3$ recorded for the maxima of the three fluorescence bands. The excitation spectrum for the violet emission exhibits a single band (*a*) peaking at 265 nm at 6.5 K, which is red shifted as the temperature increases.

The excitation spectrum for the green fluorescence comprises two distinct bands centred at 250 and 310 nm (labelled *b*), respectively, at 6.5 K. As the temperature exceeds 150 K, the (*a*) excitation band appears in the (*b*) spectrum, until becoming the preponderant band at room temperature (figure 5, curve *b*).

The excitation spectrum for the blue fluorescence (*c*) cannot be easily recorded, due to the large overlap between the violet and blue bands. Only the band peaking at 315 nm can be taken into account since the blue emission cannot be excited at a wavelength shorter than 285 nm. In addition, excitation spectra for the violet and green emissions were recorded in the vacuum UV (figure 6). In both cases, an additional band was found at 195 nm and 200 nm, respectively, at 10 K.

3.3. Decay measurements

The fluorescence decays have been measured for the violet and green emissions under 282 nm pulsed laser excitation. The temperature dependences are shown in figures 7 and 8. Above 30 K, all the decays are exponential. Below 30 K the curves can be fitted by the sum of a fast and a slow component. Only the latter has been taken into account in the description of the thermal evolution.

(i) Violet emission. The lifetime decreases rapidly between 1.6 and 25 K and more slowly until 150 K.

This behaviour is often observed in Cu^+ doped compounds and, since the early work by Pedrini [15], is usually interpreted using a model involving two close thermalized metastable levels, the lifetime of the lower being much longer than that

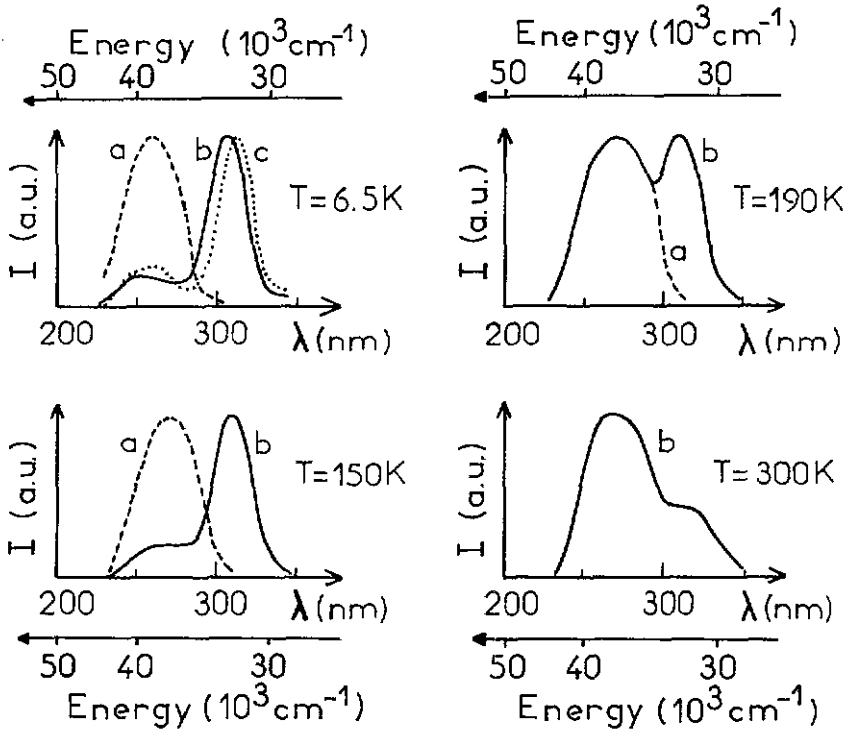

Figure 5. Thermal evolution of $CuZr_2(PO_4)_3$ excitation bands (normalized spectra): (*a*) violet emission ($\lambda_{em} = 400$ nm, broken curve), (*b*) green emission ($\lambda_{em} = 550$ nm, full curve), (*c*) blue emission ($\lambda_{em} = 460$ nm, dotted curve).

of the upper one. By solving the appropriate rate equations, the τ^{-1} fluorescence probability can be written as:

$$\tau^{-1} = [A_{31} + A_{21}\exp(-\epsilon/kT)]/[1 + \exp(-\epsilon/kT)] \qquad (1)$$

where A_{31} and A_{21} are the radiative transition probabilities between the excited states (upper level 2 and lower level 3) and the ground state (level 1) (figure 9). ϵ represents the energy mismatch between the two excited states. Between 1.6 and 150 K, the best fit to experimental data obtained from this expression gives the following results:

$$A_{31} = 5920\ s^{-1} \qquad A_{21} = 57140\ s^{-1} \qquad \epsilon = 31\ cm^{-1}.$$

In agreement with this model, the onset of a plateau below the liquid helium temperature can be surmised. This plateau is made more clearly evident by the theoretical curve (figure 7). However, above 150 K, the marked decrease of the decay constant before the luminescence is quenched at around 230 K cannot be explained by such a model. This behaviour will be discussed later.

Time-resolved spectroscopy (TRS) experiments were carried out under 282 nm pulsed laser excitation at 90 and 190 K. The spectra were recorded 0.5, 10 and 40 μs after the excitation pulse. At 90 K, only the violet fluorescence is observed, with a decreasing intensity as the delay increases. But at 190 K, both violet and green emissions coexist. The latter increases at the expense of the former which is completely quenched after 40 μs (figure 10).

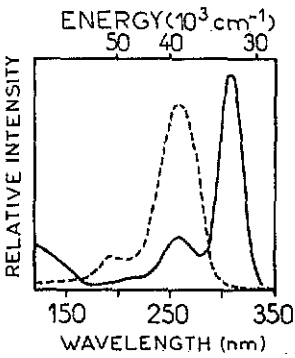

Figure 6. Excitation spectra at $T = 10$ K under synchrotron radiation excitation (LURE) for the violet emission ($\lambda_{em} = 402$ nm, broken curve) and for the green emission ($\lambda_{em} = 540$ nm, full curve).

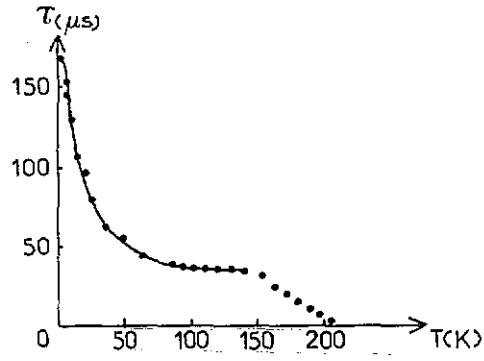

Figure 7. Variation of the violet emission decay constant versus temperature ($\lambda_{exc} = 282$ nm, $\lambda_{em} = 400$ nm). The theoretical curve (full curve) is obtained by modelling according to equation (1).

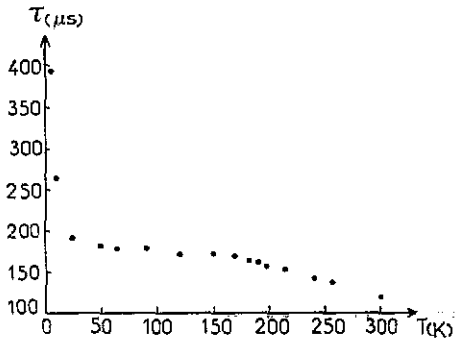

Figure 8. Evolution of the green emission decay constant as a function of temperature ($\lambda_{exc} = 282$ nm, $\lambda_{em} = 550$ nm).

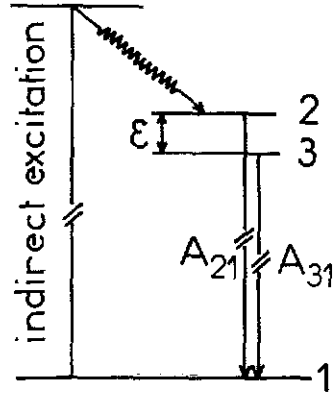

Figure 9. Three-level model for Cu^+ centres.

(ii) Green emission. The thermal evolution of the green emission decay cannot be described by a three-level system for two reasons: the lack of onset of a plateau at very low temperature, which hinders the determination of A_{31}; and the rapid decrease of τ between 4.2 and 15 K which formally leads to a value of ϵ close to zero. The TRS experiments carried out under the pulse excitation of a nitrogen laser ($\lambda_{exc} = 337$ nm) only reveal the existence of the green emission, whose intensity decreases with time.

(iii) Blue emission. The decay of the blue emission is very fast and decreases on heating from 24 ns at 4.2 K to 16 ns at 50 K.

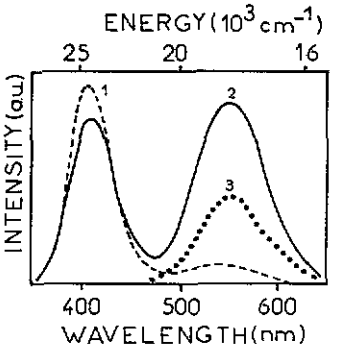

Figure 10. Time-resolved emission spectra of $CuZr_2(PO_4)_3$ at $T = 190$ K, under 282 nm laser excitation, for different delay times: (1) 0.5 μs (broken curve), (2) 10 μs (full curve), (3) 40 μs (dotted curve).

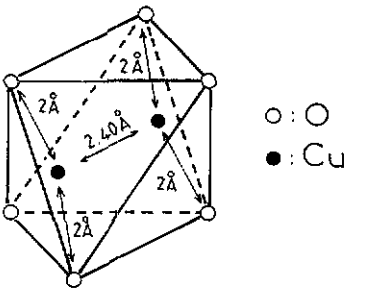

Figure 11. $(Cu^+)_2$ pair in the M(1) site [13].

4. Discussion

4.1. Origin of the luminescence

The reproducibility of the experiments was carefully checked with various samples of $CuZr_2(PO_4)_3$ and no luminescence was detected when studying the copper-free isostructural phosphate $NaZr_2(PO_4)_3$ whatever the excitation conditions or temperature. The contribution to luminescence of a hypothetical impurity can be excluded and therefore all three bands must be due to the presence of monovalent copper.

From the structural data, two possible emitting species can be inferred:

(i) single copper ions in the off-centre position of the M(1) site occupied by Na^+ in the prototype $NaZr_2(PO_4)_3$, and

(ii) pairs of copper ions located in the same M(1) site (figure 11).

4.2. Violet emission

To make the discussion easier, it is worth briefly reviewing the spectroscopic properties of isolated Cu^+ in insulating crystals or glasses. Until now, all the data have concerned copper-doped materials. Table 1 lists the emission band maximum wavelength associated with the Cu^+ luminescence and the corresponding lifetime of the emitting levels, for various luminescent compounds containing isolated Cu^+ ions. In all cases, the emission of oxides is red shifted compared to that of the alkali halides. These emission bands arise from Cu(I) monomers and can be attributed to $3d^9 4s \rightarrow 3d^{10}$ transitions. A more complete identification of the emitting levels is complicated by the off-centre localization of Cu^+ in the sites of the host material. As a general rule, the thermal evolution of the decays can be described by a three-level model. For glasses, the properties are largely dependent on the multisite structure found for the copper impurity.

In addition, in the sodium copper-doped phase $Na_{0.95}Cu_{0.05}Zr_2(PO_4)_3$, under 254 nm excitation, the violet emission still occurs, even at room temperature,

Table 1. Emission band maximum and lifetime of the emitting levels for various luminescent compounds containing isolated Cu^+ ions.

Materials	Emission band maximum (nm)	Lifetime (μs)	Reference
Crystallized			
β'' alumina: Cu^+	410, 440	33 (77 K)	17
$SrLiPO_4$: Cu^+	410		24
$BaLiPO_4$: Cu^+	450		24
NaCl: Cu^+	350	3000 (4.2 K) 40 (300 K)	3
LiCl: Cu^+	320	500 (4.2 K) 40 (300 K)	15
NaF: Cu^+	375, 390	1470 (4.2 K) 95 (300 K)	4
Glassy			
Borate $Cu^{(1)}$0.14 mole%	450	450 (4.2 K) 40 (300 K)	6
Phosphate Cu_2O 0.01 mole%	450	230 (4.2 K) 45 (300 K)	7
SiO_2 glass: Cu^+	430	Bi-exponential 40-97 (300 K)	10
Glassy SrB_4O_7	450	2024 (4.2 K) 27 (300 K)	25

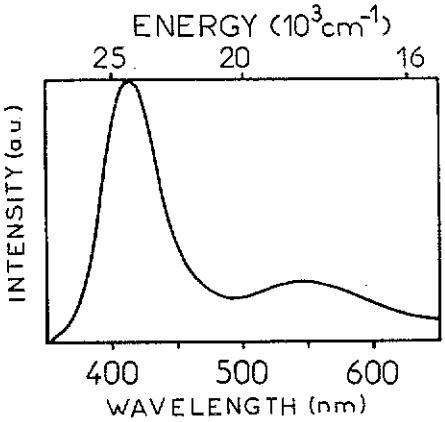

Figure 12. Emission spectrum of $Na_{0.95}Cu_{0.05}Zr_2(PO_4)_3$ at room temperature under 254 nm continuous excitation.

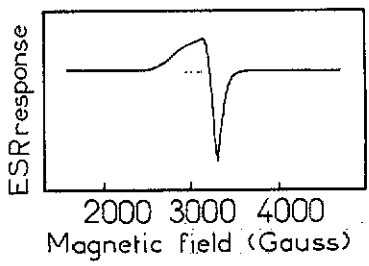

Figure 13. ESR spectrum of $CuZr_2(PO_4)_3$ at room temperature.

simultaneously with the green emission, but with a much higher intensity (figure 12). Thus the proportion of green emitting centres is much lower in this case than in that of pure copper phosphate. All these data allow us to assign the violet emission to isolated Cu^+ within the M(1) site.

4.3. Green emission

In comparison with the spectroscopic properties of the violet emitting centres, three

differences essentially characterize the green centres: firstly a lowering of the excitation and emission energies, of about 7000 cm^{-1}; secondly a large Stokes shift involving a wider electronic delocalization during the excitation process (13700 cm^{-1} for the violet centres and 17800 cm^{-1} for the green centres, at 6.5 K); and finally a longer lifetime in the investigated temperature range.

Similar dynamic evolution has been noticed for the 'white emission' of the Cu^+ dimers in the $SrCl_2$ lattice [16] and for the green emission of the Cu^+–Cu^+ pairs in copper(I)-doped $Na^+\beta''$ alumina [17]. In the latter material, copper ions are assumed to be located in the commonly labelled mO sites in the conduction planes and separated by 2.6 Å. Accordingly, the green emission of $CuZr_2(PO_4)_3$ can be attributed to the $(Cu^+)_2$ dimers existing in the M(1) site.

Copper pairing was predicted by means of molecular orbital calculations [14]: a weak attractive interaction exists as a result of a mixing of the 4s and 4p orbitals with the 3d orbitals. In this model, the lowest empty level corresponds to the σ bonding created by the two 4s orbitals and the emission transition is assumed to occur between this σ orbital and the σ antibonding orbital (AO) derived from the 3d AO. As mentioned in [14], the effect of direct Cu–Cu interaction cannot be distinguished from the influence of the ligands around the copper atoms, but the luminescence is evidence for the copper–copper bonds in such systems.

4.4. Transfer $Cu^+ \rightarrow (Cu^+)_2$

An energy transfer between these two types of centres is clearly demonstrated by the analysis of the excitation spectra, the TRS measurements and the thermal behaviour of the violet luminescence decay above 150 K.

Figure 5 shows the progressive growth of the (α)-band, characteristic of the violet emitters, in the excitation spectrum recorded for the green emission, as the temperature increases. It results from an energy transfer which is thermally activated for temperatures higher than 150 K, in accordance with the evolution of emission intensities shown in figure 2. Simultaneously, the decay constant of the violet fluorescence rapidly decreases (figure 7). The transfer is fast: e.g. at 190 K, it is completed 40 μs after the excitation pulse. At room temperature, its efficiency is quite high and a large proportion of the green emitters are excited through the violet ones (figure 5). Under a 337 nm pulsed excitation, the TRS spectra exhibit only the green emission at 90 and 190 K. Therefore, the lifetime decrease of the dimer emission observed at 170 K indicates the onset of the non-radiative thermal extinction process.

4.5. Blue luminescence

The main characteristics of the blue fluorescence are its low quenching temperature (90 K) and its very short lifetime ($\simeq$ 20 ns). Its excitation spectrum is similar to that of $(Cu^+)_2$ pairs and leads us to suppose that the blue fluorescence could be more or less related to these centres. It is unlikely that $(Cu^+)_2$ pairs could be responsible for both blue and green fluorescence. Usually, in such luminescent systems, where the excited states are strongly coupled to lattice vibrations, the emission originates from the lowest excited state, to which any excitation energy in the higher states rapidly relaxes. We therefore suppose that the blue fluorescence is due to other centres.

Impurity ions could be considered to be responsible for such fast and strong luminescence. Ce^{3+} ions, for instance, give rise to such fast fluorescence, but they have been excluded from our samples. Moreover, such a fast emission at very low temperature cannot be explained by a rapid multiphonon relaxation or an efficient energy transfer, owing to its large intensity.

We are therefore led to find other interpretations. Ag^0 and Cu^0 are well-known impurity centres in alkali halides, usually coupled with V_K centres [18, 19]. Such systems consist of a single s electron outside closed shells and they involve s↔p parity-allowed transitions, which could be in agreement with the very fast fluorescence observed. However, no Cu^0 centres were identified by the ESR technique. Furthermore, no emission associated with Ag^0 or Cu^0 was detected even at 4 K in alkali halides. In fact, the irradiation in the Ag^0 or Cu^0 absorption bands produces photoconductivity and leads to bleaching of both Ag^0 and V_K centres. Therefore the assignment of the fast blue fluorescence to Cu^0 centres much be ruled out *a priori*.

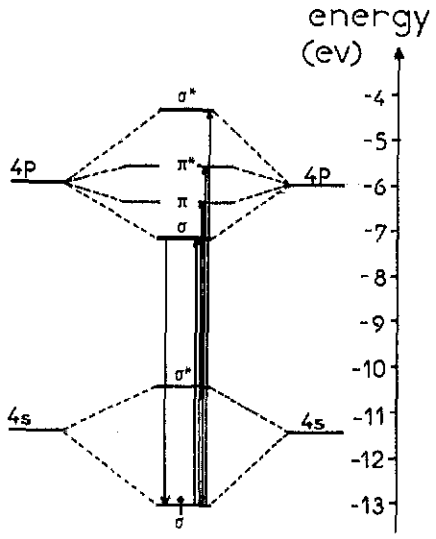

Figure 14. MO diagram proposed for a Cu_2^+ pair.

The formation of Ag_2^+ centres in silver-activated radiophotoluminescent phosphate glasses under the action of ionizing radiations has been reported [20–23]. These centres could be regarded as responsible for the orange radiophotoluminescence in these glasses. Let us examine the probability of the formation of similar Cu_2^+ centres in $CuZr_2(PO_4)_3$. In all the samples investigated, the existence of small quantities of Cu^{2+} ions was revealed unambiguously by ESR measurements (figure 13). It can be supposed that during the elaboration of the materials, an electron transfer may occur between two close Cu^+ and $(Cu^+)_2$ centres, giving rise to Cu_2^+ centres according to the following oxydo-reduction process:

$$Cu^+ \rightarrow Cu^{2+} + e^- \qquad (Cu^+)_2 + e^- \rightarrow Cu_2^+.$$

Cu_2^+ centres may be considered as Cu^+–Cu^0 pairs. The energy level diagram for Cu^+–Cu^+ pairs [14] must be modified for Cu_2^+ centres by the addition of an electron

occupying the bonding molecular orbital $\sigma(4s)$ (figure 14). As a result, the cluster should be stabilized. Qualitatively, it is clear that in this case the expected optical transitions are of parity allowed s↔p type, in agreement with the very short decay times of the blue fluorescence. It should be noted that if they exist, such Cu_2^+ centres are probably present in very weak quantities, roughly 10^4 times less than $(Cu^+)_2$ pairs. However, the strong blue fluorescence with an intensity comparable to that of the green fluorescence at low temperature can be explained by the large absorption probability which compensates for the weakness of the Cu_2^+ concentration. The correlated temperature dependences of the blue and green fluorescences at low temperature (figure 4) can be explained by an energy transfer process occurring between Cu_2^+ and $(Cu^+)_2$ centres.

5. Conclusions

The analysis of the fluorescence properties of $CuZr_2(PO_4)_3$ clearly shows the presence of two main luminescent centres exhibiting a violet emission and a green fluorescence, respectively. The violet emission is assigned to Cu^+ single ions in the M(1) site while the green emission is attributed to Cu^+–Cu^+ pairs in the same site. These assignments are in agreement with previous structural investigations using x-ray, neutron and EXAFS measurements and providing information about the location of copper ions in the network.

A third luminescence is detected in the blue range at low temperature. The origin of this fast, strong emission is not clear. It could be due to Cu^+–Cu^0 pairs in the M(1) site. Further experimentation, now in progress, is necessary to either verify this hypothesis or to find another explanation for this peculiar and interesting fluorescence.

References

[1] Simonetti J and McClure D S 1977 *Phys. Rev.* B **16** 3887
[2] Pédrini C and Jacquier B 1980 *J. Phys. C: Solid State Phys.* **13** 4791
[3] Chermette H and Pédrini C 1981 *J. Chem. Phys.* **75** 1869
[4] Moine B and Pédrini C 1984 *Phys. Rev.* B **30** 992
[5] Payne S A, Golberg A B and McClure D S 1983 *J. Chem. Phys.* **78** 3668
[6] Zhang J C, Moine B, Pédrini C, Parent C and Le Flem G 1990 *J. Phys. Chem. Solids* **51** 933
[7] Boutinaud P, Duloisy E, Pédrini C, Moine B, Parent C and Le Flem G 1991 *J. Solid State Chem.* **94** 5100
[8] Kruglik G S, Scripko G A, Shkadarevich A P, Ermolenko N N, Gorodetskaya O G, Belokon M V, Shagov A A and Zolotareva L E 1986 *J. Luminesc.* **34** 343
[9] Liu H and Gan F 1986 *J. Non-Cryst. Solids* **80** 447
[10] Debnath R and Das S K 1988 *Chem. Phys. Lett.* **155** 52
[11] Le Polles G, El Jazouli A, Olazcuaga R, Dance J M, Le Flem G and Hagenmuller P 1987 *Mat. Res. Bull.* **22** 1171
[12] Bussereau I, Belkiria M S, Gravereau P, Boireau A, Soubeyroux J L, Olazcuaga R and Le Flem G 1992 *Acta Crystallogr.* B submitted
[13] Cartier C, Dexpert H, Olazcuaga R, Bussereau I, Fargin E and Le Flem G 1992 *Eur. J. Solid State Inorg. Chem.* submitted
[14] Mehrotra P K and Hoffmann R 1978 *Inorg. Chem.* **17** 2187
[15] Pédrini C 1978 *Phys. Status Solidi* b **87** 273
[16] Payne A, Chase L L and Boatner L A 1986 *J. Luminesc.* **35** 171

[17] Barrie J D, Dunn B, Stafsudd O M and Nelson P 1987 *J. Luminesc.* **37** 303
[18] Delbecq C J, Hayes W, O'Brien M C M and Yuster P H 1963 *Proc. R. Soc.* A **271** 243
[19] Krätzig E, Timusk T and Martienssen W 1965 *Phys. Status Solidi* **10** 709
[20] Zhitnikov R A and Peregud D P 1975 *Sov. Phys.–Solid State* **17** 1080
[21] Vil'chinskaya N N, Dmitryuk A V, Ignat'ev E G, Petroskii G T and Savvina O Ch 1984 *Sov. Phys.–Solid State* **26** 497
[22] Dmitryuk A V, Karapetyan G O and Yashchurzhinskaya O A 1985 *Sov. Phys.–Solid State* **27** 1066
[23] Dmitryuk A V, Perminov A S and Savvina O Ch 1986 *Opt. Spectrosc. USSR* **60** 63
[24] Wanmaker W L and Spier H L 1962 *J. Electrochem. Soc.* **109** 109
[25] Verwey J W M, Coronado J M and Blasse G 1991 *J. Solid State Chem.* **92** 531